Eco. Env. & Cons. 26 (2) : 2020; pp. (654-662)
Copyright@ EM International
ISSN 0971–765X

Isolation of microfiber cellulose from kapok fiber (*Ceiba pentandra*) by using chemical-hydrothermal treatment

Dewi Sartika[1,2], Khaswar Syamsu[1], Endang Warsiki[1] and Farah Fahma[1]*

[1]Department of Agroindustrial Technology, Faculty of Agricultural Engineering and Technology, IPB University, 16680 Bogor, Indonesia.
[2]Department of Agribusiness, Faculty of Agricultural, Muhammadiyah University of Makassar, 90221 Makassar, Sulawesi Selatan, Indonesia

(Received 4 October, 2019; accepted 27 November, 2019)

ABSTRACT

Kapok (*Ceiba pentandra*) is one of natural fibrous sources whose potency as source of microfiber cellulose (MFC). Microfiber cellulose of kapok was isolated by chemical hydrothermal treatment and characterized by several analysis such as chemical composition analysis, scanning electron microscopy (SEM), fourier transform infrared spectroscopy (FTIR), X-ray diffraction (XRD) analyses, and thermogravimetric analysis (TGA). Kapok fiber has a high content of cellulose that is 62.87%, hemicellulose 26.32% and lignin 4.5%. The process of chemical hydrothermal treatment causes a rough fiber surface and a decrease in the size of the fiber dimensions, an increase in cellulose levels followed by a decrease in lignin and hemicellulose levels, an increase in the degree of crystallinity, and thermal stability. Because of high degree of crystallinity and thermal stability, MFC is potential to be used as a reinforcement agent in the composite matrix.

Keywords: *Kapok, Chemical-hydrothermal, Microfiber cellulose.*

Introduction

Currently, research in finding, producing, and applying eco-friendly materials based on natural fibers is advancing rapidly due to increasingly rigorous regulation on environmental issues. Various types of natural fiber have been studied and applied including frond sago fibers as adsorbents (Arnata *et al.*, 2019[a]), water hyacinth fibers as biocomposite packaging (Syafri *et al.*, 2019), jatropha shell fibers as reinforcement of PVA film composites(Manjula *et al.*, 2017), and microfiber cellulose bacteria as bone fillers (Fan *et al.*, 2013).

Kapok (*Ceiba pentandra*) is a source of natural fiber that is rarely studied. Based on the data of the Central Bureau of Statistics Indonesia on People's Plantation Production states, Indonesia is one of the largest kapok producers and exporters in the world with a total production of around 91.20 tons/year in 2015. However, the production declined each year to 52.80 tons/year in 2015 (Statistics Indonesia, 2016). Generally, kapok utilization is limited for filling material in mattresses, pillows, and dolls. Now, mattresses and pillows with kapok as fillers have been left. As the result, kapok became abundant and was not utilized well. Research on the sustainable utilization of kapok is needed so that the added value can be increased (economic value). Kapok fiber has a high cellulose content, which is around 64% (Li *et al.*, 2014), thus it has the potential as a raw

material in microfiber cellulose production. However, research and literature on the kapok utilization, especially as microfiber cellulose material, is very limited. Hence, research on microfiber isolation is still needed.

Generally, MFC is produced by chemical hydrolysis using an alkali or acidic solution. Some chemical microfiber isolations had been reported, including isolation of cellulose from frond sago with 10-15% (w/v) alkali solution for 2-3 hours (Arnata *et al.*, 2019[b]), sugarcane bagasse with 10-20% (w/v) alkali solution for 1.5-10 hours (Yue *et al.*, 2015), garlic skin with 45% sulfuric acid solution (w/v) for 2 hours at 60°C (Reddy and Rhim, 2014), rubberwood fiber with 64% H_2SO_4 at 45 °C for 1 hour (Lamaming *et al.*, 2016). The isolation process to produce cellulose with low impurities of hemicellulose and lignin requires 2-5 times process (Tanpichai *et al.*, 2019[a]). Several studies have reported that by using chemical solutions with low concentrations, which is using sodium chlorite 5% for 3 hours, could isolate the cellulose of banana fiber (Elanthikkal *et al.*, 2010). However, the application of chemical compounds containing chlorine can produce chlorine dioxide compounds which are very dangerous to the environment, so the utilization of the chlorine is prohibited. Therefore, chemical isolation tends to require higher concentration and longer processing time (Phinichka and Kaenthong, 2017).

The combination of chemical isolation with other methods can be a solution to reduce the concentration of chemical solution and processing time, one of the potential method for this combination is the hydrothermal method. The hydrothermal method is known to be eco-friendly because it requires zero catalysts, not corrosive, and efficient (Chen *et al.*, 2016[b]). Hydrothermal pre-treatment can increase the surface area of the biomass, therefore if it is combined with chemical treatment, it will facilitate accessibility and shorten the processing time (Tanpichai *et al.*, 2019[b]). On the other hand, hydrothermal treatment (HTT) requires high temperature and pressure which can damage the cellulose structure (Shi *et al.*, 2018). Hydrothermal treatment is only able to eliminate hemicellulose partially and break the lignin and hemicellulose matrix (Luz *et al.*, 2019). Therefore a combination of chemical and hydrothermal processes is needed in the isolation process to produce MFC with good physical and chemical properties.

Each isolation method produces different physical and chemical characteristics of MFC, depends on the material and the process conditions. In this regard, this study aimed to isolate the MFC of kapok fiber by using a combination of chemical and hydrothermal treatment, namely alkali hydrothermal on the delignification process and acid hydrothermal on MFC isolation process. The combination of chemical solutions with was low concentrations and hydrothermal at relatively low pressure and short time is done to avoid damage to the structure of the fiber. Analysis of the resulting MFC include chemical composition analysis, surface morphology using SEM, functional groups using FTIR, the degree of crystallinity using XRD, and thermal stability using TGA.

Experimental

Materials and Methods

Materials

Kapok fiber (KF) selected in this research was from Javanese kapok variety (*Ceiba pentandra*) obtained from Badung region, Bali, Indonesia. Chemical materials for MFC isolation used were sodium hydroxide (NaOH) and hydrogen peroxide (H_2O_2). Chemicals for assays used were sodium lauryl sulfate, disodium ethylenediaminetetraacetate (edta), sodium borate decahydrate, disodium hydrogen phosphate, 2-ethoxyethanol, sulfuric acid, and cetyltrimethylammonium bromide. All chemical substances added was analytic grade purchased from Sigma Aldrich.

Methods

Preparation of Microfiber Cellulose

The isolation of MFC from kapok was carried out in 2 stages, namely alkali hydrothermal and acid hydrothermal. The alkali treatment is based on the alkali delignification method reported by Arnata *et al.*,(2019)[b] by modifying the conventional thermal process into hydrothermal. The kapok fiber (20 g) was put into 800 mL of 5% NaOH (w/v) and autoclaved at 121°C, 1 atm, for 1 hour. Then, the fiber was rinsed to neutral pH and dried at 50 °C for 24 hours to produce delignified kapok fiber (DKF). The hydrothermal acid process is carried out using 30% hydrogen peroxide (v/v) solution. The DKF (15 g) was put into a 1 L Erlenmeyer, added 300 mL of

30% H_2O_2 (v/v) solution and autoclaved at 121°C, 1 atm, for 1 hour. After that, the fiber was rinsed with distilled water to neutral pH and dried with an oven blower at 50 °C for 24 hours to produce MFC.

Characterization of Microfiber Cellulose

Chemical composition

Kapok fiber compositions were determined by Van Soest method which consisted of Acid Detergent Fiber (ADF) fraction, Neutral Detergent Fiber (NDF), cellulose, hemicellulose, and lignin. Acid Detergent Fiber is an insoluble fraction in the acid detergent solution consisting of cellulose and lignin fraction (Council, 2000). Neutral Detergent Fiber is an insoluble fraction in a neutral detergent solution consisting of cellulose, hemicellulose, and lignin fractions. Hemicellulose levels were calculated as the difference between the content of NDF and ADF (Van Soest *et al.,* 1991).

Scanning electron microscopy

Surface morphology and dimensions of KF, DKF and MFC were characterized by using SEM (Zeiss EVO MA10). The diameter were measured by ImageJ software. Measurement aimed to define the assumed average value distribution of 100 different measurement points on MFC diameter.

Fourier transform infrared spectroscopy

Molecule functional group bonds and absorption bands were analysed by using fourier transform infrared spectroscopy (FTIR Bruker-Tensor 37). Microfiber cellulose powdered sample (2 mg) was mixed with potassium bromide powders until reaching total weight of 200 mg before shaped to be pellet. All spectra were recorded at ambient temperature with wavelengths ranging between 4000-500 cm^{-1} and resolution of 4 cm^{-1}.

Degree of crystallinity

X-ray diffraction analysis on KF, DKF and MFC were analyzed using Bruker Advance D8 with range of 2θ at temperature between 5-40°C and step of 0.02°. Powdered samples (passed 80 mesh) was irradiated with Cu Kα (λ=0.15406 nm) at 40kV and 35 mA XRD. Materials crystallinity index was measured referring to Segal *et al.,*(1959), displayed in (Eq.1).

$$CI\ \% = \left[\frac{I_{200} - I_{AM}}{I_{200}}\right] \times 100 \quad .. (1)$$

Where CI is a degree of crystallinity, I_{002} is the maximum intensity of (200) peak diffraction in unit 2θ = 22.5° which show crystalline and amorphous degree. I_{AM} is the diffraction intensity in units 2θ = 18° which illustrate the degree of amorphous.

Microfiber cellulose d-spacing size measured by using Bragg's equation (Eq. 2) and crystallites size was measured by using Scherrer's equation (Eq. 3) (Fahma *et al.,* 2011).

Bragg's equation:

$$n\lambda = 2d \sin\theta \quad .. (2)$$

Scherrer's equation:

$$L = \frac{0.9\lambda}{H \cos\theta} \quad .. (3)$$

Where L is crystallites size, λ is X-ray wavelength (0.15418 nm), H is full width at half maximum (FWHM) in radians, and θ is Bragg's angle. X-ray diffraction profile of each peak (1-10), (110), and (200) was fitted by using multiple peak fit-Origin Pro 2017 (Origin Lab Corp. US) to determine FWHM value by using Lorentz peak functional model (R^2: 0.98-0.99)

Thermogravimetric analysis (TGA)

Microfiber cellulose thermal stability is measured by using TGA (Thermo Plus TG 8120 instrument). Sample was weighed about 10 mg, then put into the crucible. Crucible containing samples was placed in the test chamber with heating from 50 °C to 600 °C and with the temperature rate of 10 °C/min and nitrogen gas flow rate of 40 mL/min.

Results and Discussion

Chemical composition

Van Soest analysis was used to determine the chemical composition of KF, DKF and MFC. The Figure 1 showed that the content of lignin and hemicellulose decreased after treatment, conversely, cellulose content increased. Kapok fiber contains 16.15% hemicellulose, 69.75% cellulose, and 9.36% lignin. The alkali-HTT caused an increase in cellulose content to 81.07%. Meanwhile, the hemicellulose and lignin content decreased to 7.43% and 3.08%, respectively. This show that the alkali-HTT is able to partially reduce hemicellulose and break the lignin matrix. Some researchers have reported that the HTT process can damage the lignin fraction which results in an increase of cellulose content (Ibbett *et al.,* 2011; Chen *et al.,* 2016[a]; Chen *et al.,*

2017). The alkali-HTT on the fiber aim to remove the fraction of lignin, wax, and oil from the cell wall surface(Luz *et al.*, 2019). Alkali hydrothermal on wheat straw was reported to be able to swell plant cell walls, degrade hemicellulose and lignin up to 73% (Sun *et al.*, 2018).

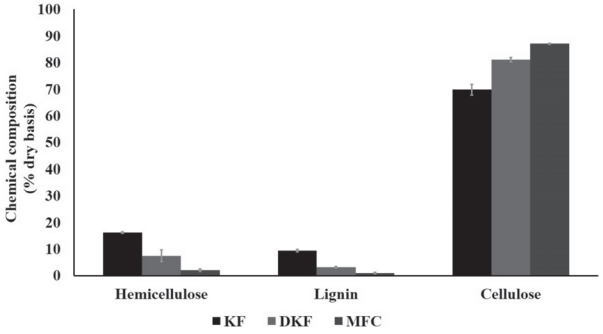

Fig. 1. Chemical composition of KF, DKF and MFC on each process stage

Furthermore, acid-HTT show the ability to increase the purity of MFC. It was evidenced by the lower hemicellulose and lignin content, which is 2.02% and 0.96%, respectively. Meanwhile, cellulose content increased to 87.06%. Acid hydrothermal using hydrogen peroxide was carried out to dissolve the remaining lignin, hemicellulose, and increase the whiteness level of MFC. The decrease in lignin and hemicellulose content was caused by the hydroperoxide anion (HOO-) in alkali media, which oxidizes the lignin structure and produces fibers with higher cellulose content and whiter color (Sun *et al.*, 2000; Tezcan and Atýcý, 2017).

Morphology and dimension of microfiber cellulose

Morphological changes in KF, DKF and MFC obtained at 250x magnification, presented in Figure 2. The morphology and dimensions of the fiber changed after alkali and acid hydrothermal treatment. Kapok fiber has a smooth surface and relatively long with a diameter of about 19.91 μm. At this stage, the natural of KF still coated by wax, lignin, and hemicellulose. The alkali-HTT make the fiber morphology become tangled because the surface structure begin to break and erode. This process is confirmed by the decrease in fiber diameter to 16.21 μm. The result is in line with the reports of Hashim *et al.*, (2017) and Ajouguim *et al.*, (2018), that the diameter of kenaf fiber decreases after alkali treatment. The morphology and surface structure of the fibers continued to change after acid-hydrothermal treatment. The acid-hydrothermal treatment produced MFC with a diameter of 12.57 μm, rough surface, and whiter color. Reduced lignin and hemicellulose fractions in the fiber caused changes in the dimensions, surface morphology, and color of the MFC. It is confirmed by the chemical composition analysis of kapok fiber and MFC in Figure 1. The MFC diameter of kapok fiber in this study is similar to the MFC diameter of coconut leaves ranging from 10-15 μm (Maheswari *et al.*, 2012), MFC from palm fruit (4-11 μm) (Reddy *et al.*, 2016), and MFC from agave (8-14 μm) (Reddy *et al.*, 2014).

Fourier transform infrared spectroscopy

Fourier transform infrared spectroscopy analysis was performed to observe changes in composition, chemical structure, and functional groups at each stage of MFC isolation. Figure 3 and Table 1 show the IR spectra of KF, DKF and MFC. In general, the

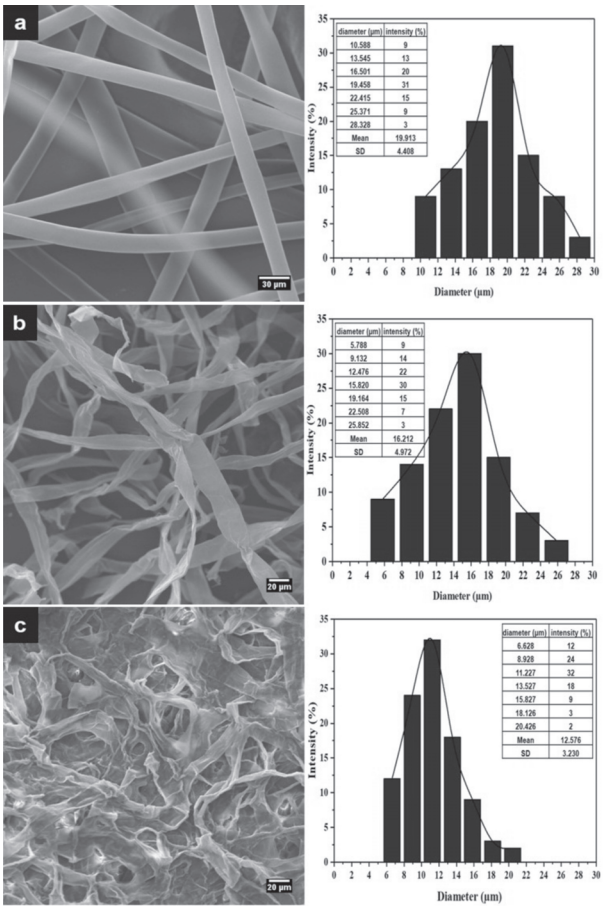

Fig. 2. SEM image results and particle size distribution of (a) KF,(b) DKF and (c) MFC

absorption band shows several similar functional groups. However, after the treatment of alkali and acid-HTT on KF shows a shifts in shape, and increased intensity of absorption bands. The spectra are relatively similar to those reported in some literature for MFC after undergo Chemical-Hydrothermal Treatment (Draman *et al.,* 2014; Mohamed *et al.,* 2017). However, there is a slight difference in intensity and shift in some of the spectral peaks. This is due to differences in the methods and conditions of the MFC isolation process. The peak around 3400 cm^{-1} shows the stretching vibrations of OH in cellulose, hemicellulose, and lignin(Maiti *et al.,* 2013). The absorption band at around 2914 cm^{-1} shows the C-H stretching vibration. The absorption intensity of KF is very small. Intensity increases in DKF and MFC after KF undergone alkali and acid-HTT. The absorption band at 1736 cm^{-1} indicates stretch C=O on hemicellulose and lignin (Natalio *et al.,* 2017; Khenblouche *et al.,* 2019). The absorption intensity in this wave is getting lower and even disappears in DKF and MFC. The same phenomenon is also shown from the absorption band 1038 cm^{-1} which indicates the vibrational deformation of the C-H bond in the aromatic ring of lignin (Bykov, 2008). This shows that alkali and acid-HTT can degrade and reduce hemicellulose and lignin. Meanwhile, peaks around 896 cm^{-1} are associated with stretching C-O-C in the β-1,4 glycosidic bonds of cellulose. This peak intensity increases with the increase in purity of cellulose after KF is treated with alkali and acid-HTT.

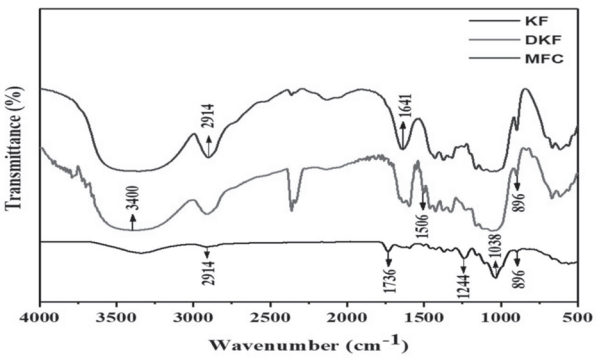

Fig. 3. FTIR spectra of KF, DKF and MFC

Degree of crystallinity

X-ray diffraction analysis was performed to determine the degree of crystallinity of KF, DKF and MFC. Alkali and acid-HTT caused an increase in the crystallinity degree and the crystallite fibes size, as shown in Figure 4 and Table 2. The amorphous phase was characterized at 2θ diffraction intensity, namely 18.50. Peaks 2θ at 15.02°, 16.27°, 22.45° and 34.60° represent the crystallographic fields of (1-10), (110), (200) and (004), showing the characteristics of the cellulose I structure (Reddy *et al.,* 2016; Ilyas *et al.,* 2017). Initial KF had a crystallinity degree of 53.6%, after the alkali and acid-HTT, it increased to 54.9% and 57.90%, respectively. The crystallinity degree of MFC from this study is relatively similar to other cellulose sources, such as dhaincha 52.8%, rice straw 53.3%, wheat straw 58.3%, corn stalks 55.3% (Nuruddin *et al.,* 2011), garlic skin 45%

Table 1. Spectra IR of KF, DKF and MFC

Wavenumber (cm^{-1})			MFC kapok		Interpretation of functional groups and types of bonds	Reference
KF	DKF	MFC	Mandal and Chakrbarty, (2014)	Mohamed *et al.,* (2017)		
3398	3400	3400	3205	3340	O-H stretching on cellulose, hemicellulose, and lignin	Maiti *et al.,* (2013)
2914	2914	2914	2894	2898	C-H stretching	Mandal and Chakrabarty, (2011)
2360	2361	2361	-	-	Asymmetric vibration of CO_2	Hosakun, (2017)
1736	-	-	-	-	C=O stretching in hemicellulose and lignin	Khenblouche *et al.,* (2019); Natalio *et al.,* (2017)
1600	1600	1641	1644	1639-1641	H-O-H deformation shows water absorption	Emandi *et al.,* (2010); Khenblouche *et al.,* (2019)
1244	1234	-	-	-	carbonyl bond of C=O ester	Zheng *et al.,* (2012)
1038	-	-			vibrational deformation of the C-H bond in the aromatic ring	Bykov (2008)
896	896	896	898	897-898	stretching at the glyosidic β-1.4 bond of cellulose	Natalio *et al.,* (2017)

(Reddy and Rhim, 2014), coconut palm leaf sheath 47.7% (Maheswari *et al.*, 2012), and sugarcane bagasse 50% (Jonjankiat *et al.*, 2011).

The increase in the crystallinity degree is caused by the degradation of the amorphous fraction of lignin, hemicellulose, and kapok fiber (Manjula *et al.*, 2017; Tian *et al.*, 2017). The d-spacing value shows the distance between the plane of the atoms, which increase to the diffraction peak. The lower d-spacing value reflects a denser and compact cellulose crystal structure (Borsoi *et al.*, 2017; Ju *et al.*, 2019). The results showed that the d-spacing values of KF, DKF and MFC in the plane (200) did not change. Meanwhile, the d-spacing value in planes (1-10) and (110) has decreased. It shows that the elimination of some amorphous fractions in the form of lignin and hemicellulose in KF causes a decrease in the d-spacing value. It is following Howwel *et al.*, (2011), who states that the hemicellulose degradation in red maple fibers contributes to changes in the d-spacing value. The changes in the d-spacing value were caused by (1) distance reduction between crystal fields due to crystal compression, (2) crystal relaxation became more active in forming compact structures, and (3) removal of non-crystalline or paracrystalline phases caused changes and tightening in crystal structure(Howell *et al.*, 2011). The crystallites dimension increased after KF undergo alkali and acid-HTT, which was 0.58 nm (KF) to 1.38 nm (DKF) and 1.94 nm (MFC). The increase in crystallite size is in parallel with the increase in the crystallinity degree. It is in line with Borsoi *et al.*,(2017) who states that an increase in crystal size can also be associated with an increase in the crystallinity degree.

Thermal stability analysis

Thermal degradation of KF, DKF, and MFC were analyzed using TGA. Thermogravimetric analysis results are presented in Figure 5. Thermal degradation of KF consisted of three stages. The first stage occurred between 50 °C - 162 °C, with a weight loss of 14.53%. The second stage occurred between 162°C-406°C, with a weight loss of 69.39%. The third stage occurred between 406 °C - 600 °C, with a weight loss of 5.91%. Thermal degradation in DKF consisted of two stages. The first stage occurs between 50 °C-363.40 °C with a weight loss of 62.96% and the second stage between 363.40 °C-600 °C with a weight loss of 13.74%. Thermal degradation in MFC consisted of two stages. The first stage between 50 °C-358 °C with a weight loss of 39.79% and the second stage between 358 °C-600 °C with a weight loss of 36.96%. In general, thermal degradation is divided into several stages. The first stage is related to the water evaporation in the fiber (Wang

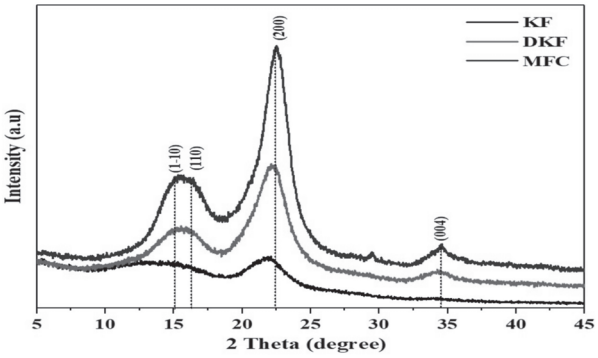

Fig. 4. XRD analytic graphs of KF, DKF and MFC

Table 2. XRD analysis results of KF, DKF and MFC

Material	d-spacing (nm)			Crystallite size (nm)			Average	CI (%)
	(1-10)	(110)	(200)	(1-10)	(110)	(200)		
KF	0.70	0.61	0.40	0.62	0.58	0.54	0.58	53.60
DKF	0.58	0.57	0.40	0.43	0.96	2.75	1.38	54.90
MFC	0.57	0.55	0.40	1.53	1.43	2.86	1.94	57.90

Table 3. Thermal characteristics of KF, DKF and MFC

Treatment	T_{onset} (°C)	T_{max} (°C)	Weight loss (%) on T_{max}	Residual char at 600 °C
KF	293.20	322.80	55.97	19.54
DKF	307.60	327.20	59.25	22.98
MFC	281.40	331.30	53.37	24.54

et al., (2014). The second stage is related to the depolymerization of hemicellulose, lignin, and cellulose (Reddy *et al.,* 2016). The third stage is heating up to 600 °C, related to the oxidation and the breakdown of carbon residues to produce low molecular weight gas (Vasconcelos *et al.,* 2017). MFC has higher thermal stability and char residue compared to KF and DKF because of MFC has a higher crystallinity degree, which confirmed by XRD analysis (Table 2), and has lower non-volatile compounds (Khenblouche *et al.*, 2019).

Derivative thermogravimetry (DTG) curves show the maximum decomposition temperature in KF, DKF, and MFC respectively 322.80 °C, 327.20 °C, and 331.30 °C. The T_{max} value in MFC is higher compared to other samples. It indicates that MFC samples are more stable against thermal degradation. Higher T_{max} values can be attributed to the characteristic of the materials that are more thermally stable (Zheng *et al.,* 2019). This value is in line with the peak value of DTG, which is shifted to a higher temperature (Broderick *et al.,* 2006). Comparison of several T_{max} MFC from various cellulose sources shows relatively similar values, such as MFC from Palmyra Palm 376°C (Reddy *et al.,* 2016), Garlic skin 341°C, onion skin 333 °C (Reddy and Rhim, 2018), Retama Raetam 311 °C (Khenblouche *et al.,* 2019), pineapple leaves 371.6 °C (Tanpichai *et al.*, 2019[b]), water hyacinth 332.71 °C (Syafri *et al.,* 2019), and Hibiscus sabdariffa 300 °C (Sonia and Dasan, 2013).

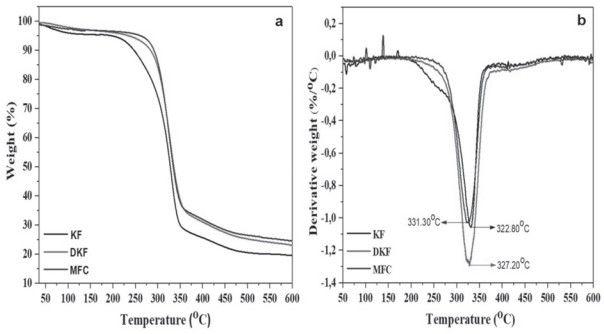

Fig. 5. TGA and DTG curve of KF, DKF and MFC

Conclusion

Kapok fiber contains cellulose of 87.06±0.14 % (dw) so it has the potential to be utilized as a source of MFC. Microfiber celllulose isolation from KF using chemical-HTT was successfully done. Chemical-HTT produces MFC with a rough surface and decreased fiber dimensions from 19.91 μm to 12.57 μm, changes in functional groups as indicators of increased cellulose purity, increase the crystallinity degree from 53.60% (KF) to 57.90% (MFC) and increase in thermal stability from 322.80 °C (KF) to 331.30 °C (MFC). Microfiber celllulose from KF has a relatively high crystallinity degree and thermal stability so it has the potential to be developed into reinforcement or fillers in the composite materials production.

Acknowledgement

The author would like to acknowledge to the Lembaga Pengelola Dana Pendidikan (The Educational Finance Administration Board - LPDP) of the Ministry of Finance of the Republic of Indonesia through a Beasiswa Unggulan Dosen Indonesia-Dalam Negeri (Indonesian Scholarship-BUDI-DN 2016 number: PRJ-6234/LPDP.3/2016) for funding this research.

References

Ajouguim, S., Abdelouahdi, K., Waqif, M., Stefanidou, M. and Saâdi, L. 2018. Modifications of Alfa fibers by alkali and hydrothermal treatment. *Cellulose.* 1-14.

Arnata, I. W., Suprihatin, S., Fahma, F., Richana, N. and Sunarti, T. C. 2019[a]. Adsorption of anionic congo red dye by using cellulose from sago frond. *Pollut. Res.* 38 : 43–53.

Arnata, I. W., Suprihatin, S., Fahma, F., Richana, N. and Sunarti, T. C. 2019[b]. Cellulose production from sago frond with alkali delignification and bleaching on various types of bleach agents. *Orient. J. Chem.* 35(1): 08-19.

Statistics Indonesia, 2016. Production of Smallholder Estate Crops by Type of Crop (thousand tons), 2000-2018.

Borsoi, C., Ornaghi, H. L., Scienza, L. C., Zattera, A. J. and Ferreira, C. A. 2017. Isolation and characterisation of cellulose nanowhiskers from microcrystalline cellulose using mechanical processing. *Polym. Polym. Compos.* 25 (8) : 563–570.

Bykov, I. 2008. Characterization of natural and technical lignins. Luleå University of Technology.

Chen, H., Yu, Y., Zhong, T., Wu, Y., Li, Y., Wu, Z. and Fei, B. 2016a. Effect of alkali treatment on microstructure and mechanical properties of individual bamboo fibers. *Cellulose.* 24 (1) : 333–347.

Chen, X., Li, H., Sun, S., Cao, X. and Sun, R. 2016b. Effect of hydrothermal pretreatment on the structural

changes of alkali ethanol lignin from wheat straw. *Scientific Reports*. 6 (1).

Chen, Y., He, Y., Fan, D., Han, Y., Li, G. and Wang, S. 2017. An efficient method for cellulose nanofibrils length shearing via environmentally friendly mixed cellulase pretreatment. *J. Nanomater.* 1–12.

Council, N. R. 2000. *Nutrient Requirements of Beef Cattle:* Seventh Revised Edition: Update 2000, Seventh Re. National Academies Press, Washington, DC.

Draman, S. S. F., Daik, R., Abdul Latif, F. and El-Sheikh, S. M. 2013. Characterization and thermal decomposition kinetics of kapok (*Ceiba pentandra* L.)–based cellulose. *Bio Resources*. 9(1).

Elanthikkal, S., Gopalakrishnapanicker, U., Varghese, S. and Guthrie, J. T. 2010. Cellulose microfibres produced from banana plant wastes: Isolation and characterization. *Carbohydr. Polym.* 80 : 852–859.

Emandi, A., Vasiliu C. I., Budrugeac, P. and Stamatin, I. 2011. Quantitative investigation of wood composition by integrated ft-ir and thermogravimetric methods. *Cellulose Chem. Technol.* 45 : 579–584.

Fahma, F., Iwamoto, S., Hori, N., Iwata, T. and Takemura, A. 2011. Effect of pre-acid-hydrolysis treatment on morphology and properties of cellulose nanowhiskers from coconut husk. *Cellulose.* 18(2) : 443–450.

Fan, X., Zhang, T., Zhao, Z., Ren, H., Zhang, Q., Yan, Y. and Lv, G. 2012. Preparation and characterization of bacterial cellulose microfiber/goat bone apatite composites for bone repair. *J. Appl. Polym. Sci.* 595–603.

Hashim, M. Y., Amin, A. M., Marwah, O. M. F., Othman, M. H., Yunus, M. R. M. and Chuan Huat, N. 2017. The effect of alkali treatment under various conditions on physical properties of kenaf fiber. *J. Phys.* 914, 1-15.

Hosakun, Y. 2017. ATR-FTIR study of the interaction of CO 2 with bacterial cellulose-based membranes, University of Sopron.

Howell, C., Hastrup, A. C. S., Jara, R., Larsen, F. H., Goodell, B. and Jellison, J. 2011. Effects of hot water extraction and fungal decay on wood crystalline cellulose structure. *Cellulose.* 18(5) : 1179-1190.

Ibbett, R., Gaddipati, S., Davies, S., Hill, S. and Tucker, G. 2011. The mechanisms of hydrothermal deconstruction of lignocellulose: New insights from thermal–analytical and complementary studies. *Bioresour. Technol.* 102 : 9272–9278.

Ilyas, R. A., Sapuan, S. M., Ishak, M. R. and Zainudin, E. S. 2017. Effect of delignification on the physical, thermal, chemical, and structural properties of sugar Palm fibre. *Bioresourc.* 12(4) : 8734-8754.

Jonjankiat, S., Wittaya, T. and Sridach, W. 2011. Improvement of Poly (vinyl alcohol) adhesives with cellulose microfibre from sugarcane bagasse. *Iran Polym J*. 20: 305–317.

Ju, X., Bowden, M., Brown, E. E. and Zhang, X. 2015. An improved X-ray diffraction method for cellulose crystallinity measurement. *Carbohydr. Polym.* 123 : 476–481.

Khenblouche, A., Bechki, D., Gouamid, M., Charradi, K., Segni, L., Hadjadj, M. and Boughali, S. 2019. Extraction and characterization of cellulose microfibers from Retama raetam stems. *Polímeros*. 29 (1) : 1–8.

Lamaming, J., Sharudin, N. H., Hashim, R. and Sulaiman, O. 2016. Characterization of cellulose microfibers isolated from rubberwood (*Hevea brasiliensis*). *Int. J. Adv. Sci. Eng. Inf. Technol.* 6 (2) : 170-174.

Li, M., Cheng, Y.-L., Fu, N., Li, D., Adhikari, B. and Chen, X. D. 2014. Isolation and characterization of corncob cellulose fibers using microwave-assisted chemical treatments. *Int. J. Food. Eng.* 10 (3) : 427–436.

Luz, J. D., Losekann, M. A., Santos, A. dos, Halison de Oliveira, J., Girotto, E. M., Moises, M. P., Radovanovic, E. and Fávaro, S. L. 2019. Hydrothermal treatment of sisal fiber for composite preparation. *J. Compos. Mater.* 1-11.

Nuruddin, M., Chowdhury, A., Haque, S.A., Rahman, M., Farhad, S.F., Jahan, M.S. and Quaiyyum, A. 2011. Extraction and characterization of cellulose microfibrils from agricultural wastes in an integrated biorefinery initiative. *Cellulose Chem. Technol.* 45 : 347–354.

Maheswari, C. U., Obi Reddy, K., Muzenda, E., Guduri, B. R. and Rajulu, A. V. 2012. Extraction and characterization of cellulose microfibrils from agricultural residue – *Cocos nucifera* L. *Biomass and Bioenergy*. 46: 555–563.

Maiti, S., Jayaramudu, J., Das, K., Reddy, S. M., Sadiku, R., Ray, S. S. and Liu, D. 2013. Preparation and characterization of nano-cellulose with new shape from different precursor. *Carbohydr Polym*. 98 : 562–567.

Mandal, A. and Chakrabarty, D. 2011. Isolation of nanocellulose from waste sugarcane bagasse (SCB) and its characterization. *Carbohydr. Polym.* 86 : 1291–1299.

Manjula, P., Srinikethan, G. and Shetty K. V. 2017. Biocomposite composed of PVA reinforced with cellulose microfibers isolated from biofuel industrial dissipate; *Jatropha Curcus* L seed shell. *J. Environ. Chem. Eng.* 5(2) : 1990–1997.

Mohamed, M. A., W. Salleh, W. N., Jaafar, J., Ismail, A. F., Abd Mutalib, M., Mohamad, A. B., Zain,M. F.M., Awang, N.A. and Mohd Hir, Z. A. 2017. Physicochemical characterization of cellulose nanocrystal and nanoporous self-assembled CNC membrane derived from *Ceiba pentandra*. *Carbohydr. Polym.* 157: 1892–1902.

Natalio, F., Fuchs, R., Cohen, S. R., Leitus, G., Fritz-Popovski, G., Paris, O., Kappl, M. and Butt, H.J. 2017. Biological fabrication of cellulose fibers with tailored properties. *Science.* 357 (6356) : 1118–1122.

Phinichka, N. and Kaenthong, S. 2017. Regenerated cellulose from high alpha cellulose pulp of steam-exploded sugarcane bagasse. *J. Mater. Res. Technol.* 7(1): 55–65.

Reddy, J. P. and Rhim, J. 2014. Isolation and characterization of cellulose nanocrystals from garlic skin. *Mater. Lett*. 1-4.

Reddy, J. P. and Rhim, J. 2018. Extraction and characterization of cellulose microfibers from agricultural wastes of onion and garlic extraction and characterization of cellulose microfibers from. *J. Nat. Fibers.* 1–9.

Reddy, K. O., Maheswari, C.U., Dhlamini, M.S. and Kommula, V. P. 2016. Exploration on the characteristics of cellulose microfibers from *Palmyra palm* fruits. *Int. J. Polym. Anal. Charact.* 21(4) : 286–295.

Reddy, K. O., Zhang, J., Zhang, J. and Rajulu, A. V. 2014. Preparation and properties of self-reinforced cellulose composite films from agave microfibrils using an ionic liquid. *Carbohydr. Polym.* 114 : 537–545.

Segal, L., Creely, J. J., Martin, A. E. and Conrad, C. M. 1959. An empirical method for estimating the degree of crystallinity of native cellulose using the x-ray diffractometer. *Text. Res. J.* 29 (10) : 786–794.

Shi, J., Lu, Y., Zhang, Y., Cai, L. and Shi, S. Q. 2018. Effect of thermal treatment with water, H_2SO_4 and NaOH aqueous solution on color, cell wall and chemical structure of poplar wood. *Sci. Report*. 8(1).

Sonia, A. and Dasan, K. P. 2013. Chemical, morphology and thermal evaluation of cellulose microfibers obtained from *Hibiscus sabdariffa*. *Carbohydr. Polym.* 92(1) : 668–674.

Sun, R. C., Tomkinson, J., Ma, P. L. and Liang, S. F. 2000. Comparative study of hemicelluloses from rice straw by alkali and hydrogen peroxide treatments. *Carbohydr. Polym.* 42 (2) : 111–122.

Sun , S., Zhang, L., Liu, F., Fan, X. and Sun, R. C. 2018. One-step process of hydrothermal and alkali treatment of wheat straw for improving the enzymatic saccharification. *Biotechnol. Biofuels.* 11 (137) : 1-10.

Syafri, E., Jamaluddin, Wahono, S., Irwan, A., Asrofi, M., Sari, N. H. and Fudholi, A. 2019. Characterization and properties of cellulose microfibers from water hyacinth filled sago starch biocomposites. *Int. J. Biol. Macromol*. 137 : 119–125.

Tanpichai, S., Boonmahitthisud, A. and Witayakran, S. 2019[a]. Use of steam explosion as a green alternative method to prepare pulp from pineapple leaves. *J. Met. Mater. Miner.* 29(2) : 110-114.

Tanpichai, S., Witayakran, S. and Boonmahitthisud, A. 2019[b]. Journal of Environmental chemical engineering study on structural and thermal properties of cellulose micro fi bers isolated from pineapple leaves using steam explosion. *J. Environ. Chem. Eng*. 7 : 102836.

Tezcan, E. and Atici, O. G. 2017. A new method for recovery of cellulose from lignocellulosic bio-waste: Pile processing. *Waste Manag.* 70 : 181–188.

Tian, D., Chandra, R. P., Lee, J. S., Lu, C. and Saddler, J. N. 2017. A comparison of various lignin-extraction methods to enhance the accessibility and ease of enzymatic hydrolysis of the cellulosic component of steam-pretreated poplar. *Biotechnol. Biofuels.* 10 : 157: 1-10.

Soest, P. J. V., Robertson, J. B. and Lewis, B. A. 1991. Methods for dietary fiber, neutral detergent fiber, and nonstarch polysaccharides in relation to animal nutrition. *J. Dairy Sci.* 74 : 3583–3597.

Vasconcelos, N. F., Feitosa, J. P. A., da Gama, F. M. P., Morais, J. P. S., Andrade, F. K., de Souza Filho, M. de S. M. and Rosa, M. de F. 2017. Bacterial cellulose nanocrystals produced under different hydrolysis conditions: Properties and morphological features. *Carbohydr. Polym.* 155 : 425–431.

Wang, T., Xu, X., Ren, Y., Qin, S., Sui, X. and Wang, L. 2014. Kinetics of thermal degradation of viscose fiber and fire retardant viscose fiber. *J. Eng. Fibers Fabr*. 9 (2) : 28-46.

Yue, Y., Han, J., Han, G., Aita, G. M. and Wu, Q. 2015. Cellulose fibers isolated from energycane bagasse using alkali and sodium chlorite treatments: Structural, chemical and thermal properties. *Ind. Crop. Prod.* 76 : 355–363.

Zheng, C., Li, D. and Ek, M. 2018. Mechanism and kinetics of thermal degradation of insulating materials developed from cellulose fiber and fire retardants. *Journal of Thermal Analysis and Calorimetry. J. Therm. Anal. Calorim.* 135 : 3015–3027.

Zheng, Y., Wang, W., Huang, D. and Wang, A. 2012. Kapok fiber oriented-polyaniline nanofibers for efficient Cr (VI) removal. *Chem. Eng. J.* 191 : 154–161.